Quantum antiferromagnetic Heisenberg half-odd-integer spin model as the entanglement Hamiltonian of the integer-spin Affleck-Kennedy-Lieb-Tasaki states

Wen-Jia Rao, Guang-Ming Zhang, and Kun Yang

Phys. Rev. B **93**, 115125 — Published 15 March 2016

DOI: 10.1103/PhysRevB.93.115125

Quantum antiferromagnetic Heisenberg half-odd integer spin model as the entanglement Hamiltonian of the integer spin Affleck-Kennedy-Lieb-Tasaki states

Wen-Jia Rao[1] and Guang-Ming Zhang[1,2*] and Kun Yang[3]
[1] *State Key Laboratory of Low-Dimensional Quantum Physics and Department of Physics, Tsinghua University, Beijing 100084, China.*
[2] *Collaborative Innovation Center of Quantum Matter, Beijing 100084, China.*
[3] *National High Magnetic Field Laboratory and Physics Department, Florida State University, Tallahassee, Florida 32310, USA.*
(Dated: February 24, 2016)

Applying a symmetric bulk bipartition to the one-dimensional Affleck-Kennedy-Lieb-Tasaki valence bond solid (VBS) states for the integer spin-S Haldane gapped phase, we can create an array of fractionalized spin-S/2 edge states with the super unit cell l in the reduced bulk system, and the topological properties encoded in the VBS wave functions can be revealed. The entanglement Hamiltonian (EH) with $l = even$ corresponds to the quantum antiferromagnetic Heisenberg spin-S/2 model. For the even integer spins, the EH still describes the Haldane gapped phase. For the odd integer spins, however, the EH just corresponds to the quantum antiferromagnetic Heisenberg half-odd integer spin model with spinon excitations, characterizing the critical point separating the topological Haldane phase from the trivial gapped phase. Our results thus demonstrate that the topological bulk property not only determines its fractionalized edge states, but also the quantum criticality associated with the topological phase, where the elementary excitations are precisely those fractionalized edge degrees of freedom *confined* in the bulk of the topological phase.

PACS numbers: 05.30.Rt, 05.30.-d, 03.65.Vf

I. INTRODUCTION

Topological phases of matter including those require symmetry protection have been the subject of intense interest in quantum information science, condensed matter physics and quantum field theory. Much effort has been devoted to classification of these topological phases, and tremendous success is achieved in our understanding of quantum Hall states[1], topological insulators[2–4], and symmetry protected topological (SPT) phases[5–7]. The SPT phases possess bulk energy gaps and do not break any symmetry, but have robust gapless edge excitations. These SPT states can not be continuously connected to a trivial gapped state without closing the energy gap. So there exists a topological phase transition between a SPT phase and its adjacent trivial phase, and the corresponding critical theory does not belong to the conventional Landau-Ginzburg-Wilson paradigm[8–11]. Such a critical point is a prototype of "deconfined quantum critical point (QCP)" with fractionalized elementary excitations[12]. A crucial question is how to extract the critical properties from the ground state wave function of the SPT phases.

In one dimension, Haldane[13] predicted that quantum antiferromagnetic Heisenberg spin chains are classified into two universality classes: half-odd integer spins with gapless excitations and integer spins with gapped excitations. Recent studies[14, 15] indicated that the Haldane gapped phase for *odd* integer spin chains is a typical SPT phase, while the *even* integer spin chains correspond to the topologically trivial phase, because their edge states are not protected by the projective representation of the bulk SO(3) symmetry. According to the classification theory[7], there exists only one nontrivial SPT phase for the SO(3) symmetric quantum Heisenberg spin model, whose fixed point wave function is given by the Affleck-Kennedy-Lieb-Tasaki (AKLT) valence bond solid state (VBS)[16]. Since the symmetry protection of the SPT phase in the bulk can be analyzed in terms of symmetry protection of the fractionalized edge spins, it motivates us to question if there exists a general connection between the SPT phase and the quantum critical phases of the quantum antiferromagnetic Heisenberg half-odd-integer spin chains.

In this paper, we first review the entanglement property of a single block in the one-dimensional integer spin-S AKLT VBS states, and prove that the entanglement Hamiltonian can be expressed in terms of the Heisenberg exchange of two edge spin-S/2's. By using a symmetric bulk bipartition[9, 17, 18], we can create an array of fractionalized spin-S/2 edge states with super unit cell l in the reduced bulk system. Then the reduced density matrix and entanglement Hamiltonian (EH) can be derived in terms of the fractionalized edge spins, leading to the quantum antiferromagnetic Heisenberg spin-S/2 model when the super unit cell l includes even number of lattice sites. For $S = 4n + 2$ with integer n, the EH still describes the nontrivial Haldane gapped phase with odd integer spins, and for $S = 4n$ the EH corresponds to the even integer Haldane gapped phase. For the odd integer spin-S, however, the quantum antiferromagnetic Heisenberg half-odd integer spin model emerges, characterizing the quantum critical point separating the nontrivial Haldane phase from the trivial phase. So our re-

sults demonstrate that the topological bulk property not only determines its fractionalized edge states, but also the critical point at the continuous phase transition to its nearby trivial phase.

II. SINGLE BLOCK ENTANGLEMENT

The spin-S AKLT VBS state as the fixed point state of the Haldane gapped phase is defined by

$$|\text{VBS}\rangle = \prod_{i=0}^{N} \left(a_i^\dagger b_{i+1}^\dagger - b_i^\dagger a_{i+1}^\dagger\right)^S |vac\rangle, \tag{1}$$

where $a_i^\dagger$ and $b_i^\dagger$ are the Schwinger boson creation operators with a local constraint $a_i^\dagger a_i + b_i^\dagger b_i = 2S$, and the spin operators are expressed as $S_i^+ = a_i^\dagger b_i$, $S_i^- = b_i^\dagger a_i$, and $S_i^z = \left(a_i^\dagger a_i - b_i^\dagger b_i\right)/2$. In this construction, each physical spin is composed of two spin-$S/2$'s projected into a total spin-S state, while each neighboring sites are linked by spin-$S/2$ singlet, see Fig. 1(a).

To consider the entanglement properties, we choose a block of l sites denoted by the part A. With the help of the spin coherent state representation, the reduced density matrix ρ_A can be obtained by tracing out the degrees of freedom without the part A, and its nonzero eigenvalues λ_j with degeneracy $2j+1$ have been derived[19, 20]

$$\begin{aligned}\lambda_j &= \frac{1}{(S+1)^2}\sum_{k=0}^{S}(2k+1)\left[f(k)\right]^{l-1} \\ &\quad \times I_k\left[\frac{1}{2}j(j+1) - \frac{1}{4}S(S+2)\right], \end{aligned}\tag{2}$$

$$f(k) = \frac{(-1)^k S!\,(S+1)!}{(S-k)!\,(S+k+1)!}, \tag{3}$$

where $j = 0, 1, ...S$ and the recursion function $I_k[x]$ is defined by

$$\begin{aligned}I_{k+1}[x] &= \frac{2k+1}{(S+k+2)^2}\left(k + \frac{4x}{k+1}\right) I_k[x] \\ &\quad - \frac{k}{k+1}\left(\frac{S-k+1}{S+k+2}\right)^2 I_{k-1}[x], \end{aligned}\tag{4}$$

with $I_0[x] = 1$ and $I_1[x] = \frac{4x}{(S+2)^2}$. Since the function $|f(k)|$ decreases with k very quickly, only the first two terms ($k = 0, 1$) dominate in the summation for a long block length l. Thus the eigenvalues are approximated as

$$\lambda_j \approx \frac{1}{(S+1)^2} + 3\left(\frac{-S}{S+2}\right)^{l-1}\frac{\left[2j(j+1) - S(S+2)\right]}{(S+2)^4},$$

and up to the first order of $\delta = \left(\frac{-S}{S+2}\right)^l$ the entanglement spectrum is thus derived as

$$\xi_j \approx J(l)\left[\frac{1}{2}j(j+1) - \frac{S}{2}\left(\frac{S}{2}+1\right)\right], \tag{5}$$

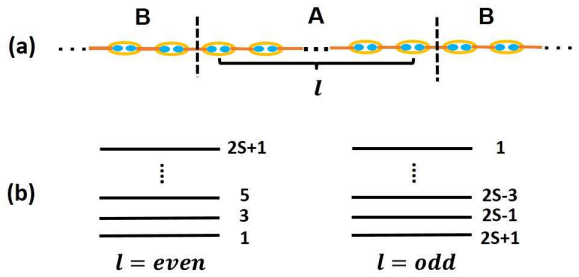

FIG. 1: (a) The picture of AKLT VBS state. Each blue dot represents a spin-$S/2$, yellow circle stands for the physical spin-S, and solid lines denote the singlet bonds. A block with l sites is chosen as the subsystem A. (b) The entanglement spectra of the single block are given for l =even and l =odd, respectively.

with $J(l) = \frac{12}{S(S+2)}\left(\frac{-S}{S+2}\right)^l$. Then the corresponding EH can be recognized as: $H_E = J(l)\,\mathbf{s}_1 \cdot \mathbf{s}_2$ where $\mathbf{s}_1$ and $\mathbf{s}_2$ are the fractionalized edge spins. Therefore, for a long block length l, the entanglement properties of the single block are just described by the quantum Heisenberg spin model, and the corresponding entanglement spectra are displayed in Fig. 1(b).

III. SYMMETRIC BULK BIPARTITION

The symmetric bulk bipartition is the most effective tool to generate an extensive array of fractionalized edge spin-S/2's in the bulk subsystem, i.e., the spin chain is divided into two subsystems both including the same number of disjoint blocks[9, 17]. The fractionalized edge spins can thus percolate in the reduced bulk system and emerge as coherent elementary excitations of the effective field theory of the subsystem. It is convenient to write the AKLT VBS wave function in the form of matrix product state (MPS) representation shown in Fig. 2(a)

$$|VBS\rangle = \sum_{\{s_i\}} \text{Tr}\left[A^{[s_1]}A^{[s_2]}..A^{[s_N]}\right]|s_1, s_2, ..s_N\rangle, \tag{6}$$

where $A^{[s_i]}$ are the $(S+1)\times(S+1)$ local matrices, whose elements can be obtained from the Schwinger boson representation, and the periodic boundary condition are assumed. When we group each continuous l lattice sites into a block, all the even blocks are denoted by the part A and the rest by the part B. Then by tracing out the part B, the reduced density matrix ρ_A and the EH ($H_E = -\ln\rho_A$) can be derived. The general procedure is described as the following four steps.

Step 1. Conduct the coarse graining and distill relevant states within each block[21]. We pick out a block with l

sites, and perform the singular value decomposition

$$\left(A^{[s_1]}A^{[s_2]}..A^{[s_l]}\right)_{\alpha,\beta} = \sum_{p=0}^{\kappa-1} X_{(\{s_i\}),p}\Lambda_p Y_{p,(\alpha,\beta)}, \quad (7)$$

where the number of nonzero singular values κ records the number of relevant states in the block. For the spin-S AKLT VBS state, $\kappa = (S+1)^2$, and the relevant states $|p\rangle$ are effectively composed by two edge spin-$S/2$'s:

$$|p\rangle = \sum_{m,n} \chi^p_{m,n}|m,n\rangle,$$

which are the combination of the degenerate edge states $|m,n\rangle$ with $m,n \in [-S/2, S/2]$. Then we can rewrite the original VBS wave function into the blocked MPS form, see Fig. 2(b)

$$|\Psi\rangle = \sum_{\{p_i\}} \mathrm{Tr}\left(B^{[p_1]}B^{[p_2]}..B^{[p_{N/l}]}\right)|p_1,p_2,..p_{N/l}\rangle, \quad (8)$$

where the block matrices are given by $B^{[p]}_{\alpha,\beta} = \Lambda_{p,p}Y_{p,(\alpha,\beta)}$.

Step 2. Trace out the degrees of freedom in the part B. Such a procedure can be presented elegantly by a graphical notation described in Fig. 2(c). The contribution of the subsystem B is represented by the transfer matrix $T = \sum_p B^{[p]} \otimes \bar{B}^{[p]}$. The expression ρ_A can be written into a matrix product operator form, which is displayed in Fig. 2(c)

$$\rho_A = Tr\left(\prod_j R_j\right), \quad (9)$$

$$R_j = \sum_{p_j,q_j} |p_j\rangle\langle q_j|\left(B^{[p_j]} \otimes \overline{B}^{[q_j]}\right)T. \quad (10)$$

Step 3. To derive the EH, we have to express the projection operator $|p_j\rangle\langle q_j|$ in terms of product of spin operators. Note that each $|p_j\rangle$ is composed of two spin-$S/2$'s and we can write an expansion:$|m\rangle\langle n| = \sum_i \Gamma_{(m,n),i}O^i$, where O^i $(i = 0,1,...S^2+2S)$ are the spin-$S/2$ operators with $O^0 = I$. With these considerations, the full expression R_j is written as

$$R_j = \sum_{\{p_j,q_j\}}\sum_{\{m,n,\alpha\}}\left[\left(B^{[p_j]} \otimes \overline{B}^{[q_j]}\right)T\right]\chi^{p_j}_{m_1,m_2}\overline{\chi}^{q_j}_{n_1,n_2} \times\Gamma_{(m_1,n_1),\alpha_{2j-1}}\Gamma_{(m_2,n_2),\alpha_{2j}}O^{\alpha_{2j-1}}O^{\alpha_{2j}}. \quad (11)$$

It is emphasized that no approximation has been made so far.

Step 4. Since the form R_j is complicated, a controlled approximation can be introduced. For a long block length l, the only dominant coupling in ρ_A is $\delta = \left(\frac{-S}{S+2}\right)^l$, which implies that the exchange coupling between two edge spins decays exponentially. Then R_j can be separated into two individual edge spins, and the final result for H_E is given by

$$H_E \approx \frac{12}{S(S+2)}\left(\frac{-S}{S+2}\right)^l \sum_i \mathbf{s}_i \cdot \mathbf{s}_{i+1}, \quad (12)$$

where $\mathbf{s}_i$ is the fractionalized edge spin-$S/2$'s in the reduced system. The detailed derivations for the $S=1$ and $S=2$ cases are included in the Appendix A and B.

Therefore, the resulting entanglement properties can be divided into three categories: (i) For $l = odd$, H_E represents a ferromagnetic ordered phase with spin wave excitations; (ii) For $l = even$ and $S = even$, H_E describes the Haldane gapped phase with integer spins. In particular, for $S = 4n+2$ with integer n, it represents the SPT phase of the odd integer spin Haldane phase even though the original VBS state corresponds to the topologically *trivial* state. (iii) For $l = even$ and $S = odd$, H_E is just the quantum Heisenberg antiferromagnetic half-odd integer spin model with quantum critical ground state[22]. The corresponding effective field theory for $S > 1$ describes a multicritical point characterized by the 1+1 (space-time) dimensional SU(2) level-S Wess-Zumino-Witten (WZW) theory, but the stable fixed point of these critical phases is determined by the SU(2) level-1 WZW theory[22, 23]. These are the important properties encoded in the AKLT VBS states with integer spins.

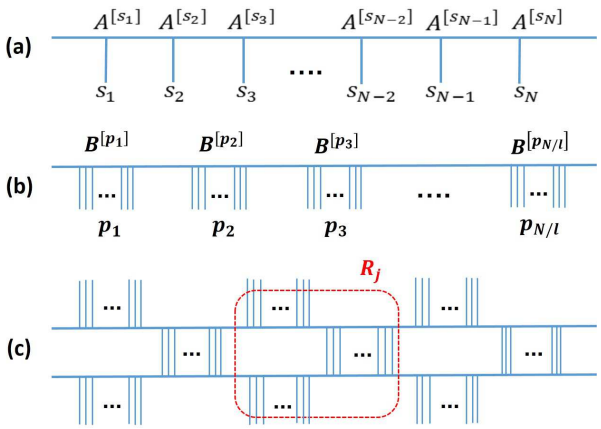

FIG. 2: (a) The MPS representation of the AKLT VBS state. (b) The blocked AKLT VBS state. (c) The reduced density matrix under symmetric bulk bipartition with a repeating structure.

IV. NUMERICAL SUPPORTS

A. Spin-1 AKLT state

In order to put the above analytical results on a solid ground, we perform the exact numerical diagonalization for the reduced density matrix ρ_A for the spin-1 AKLT

state *without* any approximations. The full entanglement spectrum (ES) for the block length $l = 4$ is displayed in Fig. 3(a). We use the effective length L_A to denote the reduced system length, independent of the block length in the original scale. The degeneracies of each levels correspond to $1, 3, 5$,etc for every system length. The density of entanglement entropy S_A/L_A saturates to 0.6929 very quickly, close to the value $\ln 2 = 0.6931$. The entanglement spectral gap $\xi_1 - \xi_0$ is found to scale linearly with the inverse subsystem length $\xi_1 - \xi_0 = k_1 L_A^{-1}$ shown in Fig. 3(b), suggesting the bulk ES is gapless in the thermodynamic limit. Moreover, the second excited entanglement level is also fitted as $\xi_2 - \xi_0 = k_2 L_A^{-1}$ displayed in Fig. 3(b), and the ratio of these two excited levels is determined as $k_2/k_1 = 1.975 \sim 2$, implying the difference of scaling dimensions for these two excited levels is 2.

To determine the universality class of this spectrum, we focus on the wave function of the lowest level $|\psi_0\rangle$. By further cutting the reduced system into two halves with lengths l_a and $(L_A - l_a)$, respectively, we calculate the entanglement entropy: $s(l_a, L_A) = \mathrm{Tr}_{l_a+1, l_a+2..L_A}(|\psi_0\rangle\langle\psi_0|)$. Fitting to the Calabrese-Cardy formula[24],

$$s(l_a, L_A) = \frac{c}{3} \ln \left[\frac{L_A}{\pi} \sin \left(\frac{\pi l_a}{L_A} \right) \right] + s_0, \qquad (13)$$

we obtain the central charge $c = 1.02 \pm 0.02$ in Fig. 3(c). This result confirms that the obtained ES belongs to the universality class of the 1+1 (space-time) dimensional $SU(2)_1$ WZW conformal field theory, which is the same as the quantum antiferromagnetic Heisenberg spin-1/2 chain. The corresponding EH describes the critical point separating the spin-1 Haldane phase from the trivial gapped phase[9]. Such a critical point differs the critical point between the Haldane phase and dimerized phase in the SO(3) bilinear-biquadratic spin-1 chain from that the dimerized phase has spontaneously translation symmetry breaking[25]. It is a multicritical point described by the 1+1 dimensional $\mathrm{SU}(2)_2$ WZW theory with $c = 3/2$.

However, when the block includes the odd number of lattice sites, e.g. $l = 3$, the bulk ES is calculated and displayed in Fig. 4(a). The entanglement entropy density is found to saturate to 0.691, which is within 0.3% to the value of $\ln 2$. The lowest entanglement level ξ_0 is linear with system size. However, the lowest entanglement level has the degeneracy $L_A + 1$ in each system size. We computed the magnetization distribution $m^z_{tot} = \sum_i m^z_i$ for these states and found they are well located in $[-L_A/2, L_A/2]$, indicating that a large spin-$L_A/2$ is formed. This can only be achieved in the ferromagnetic interacting between edge spins, and the bulk ES thus describes a ferromagnetical long-range ordered state. For more evidence, we evaluate the entanglement gap scales as $\xi_1 - \xi_0 \sim L_A^{-2}$, which is a direct sign of spin-wave excitations. To further confirm the this spectrum, we fit the second excitation level $\xi_2 - \xi_0 \sim L_A^{-2}$,

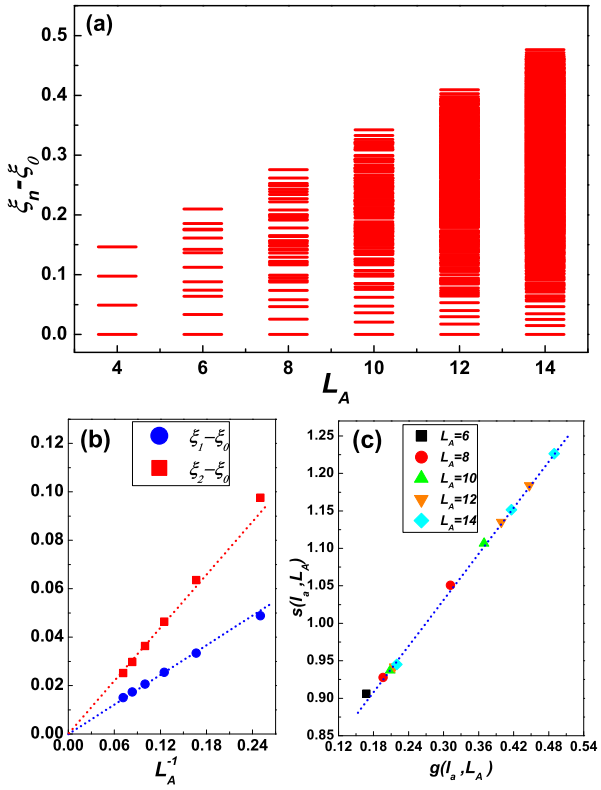

FIG. 3: (a) Bulk ES with $S = 1$ and the block length $l = 4$. (b) Two lowest entanglement levels are linear with L_A^{-1}. (c) The entanglement entropy $s(l_a, l_A)$ as a function of $g(l_a, L_A) = \frac{1}{3} \ln \left[\frac{L_A}{\pi} \sin \left(\frac{\pi l_a}{L_A} \right) \right]$.

as dictated in Fig. 4(b). If we take the Heisenberg interaction as the EH, the coupling constant is fitted to be $J \sim -0.037$, while in our analytical analysis it is $J = (-1/3)^3 = -0.038$. Thus, our analytical derivation is confirmed.

B. Spin-2 AKLT state

Another important calculation is performed for the spin-2 AKLT VBS state. The ES with $l = 6$ under *open* boundary condition is presented in Fig. 5(a). The lowest level is singlet and the first excited level is triplet. However, the level spacing between these two states is fitted as an exponential decay with the subsystem size: $(\xi_1 - \xi_0)/J(l) \sim e^{-L_A/\Delta}$ with $\Delta = 4.769$, displayed in Fig. 5(b). Here the antiferromagnetic Heisenberg coupling strength $J(l)$ is fitted to be 0.0230, very close to our analytical value 0.0234. In the thermodynamic limit, the lowest entanglement level becomes four-fold degenerate. These results are consistent with the defining property of the topological spin-1 Haldane phase. Moreover, $(\xi_2 - \xi_0)/J(l)$ shown in Fig. 5(c) approaches to the finite value 0.274, smaller than the Haldane gap value 0.41 from

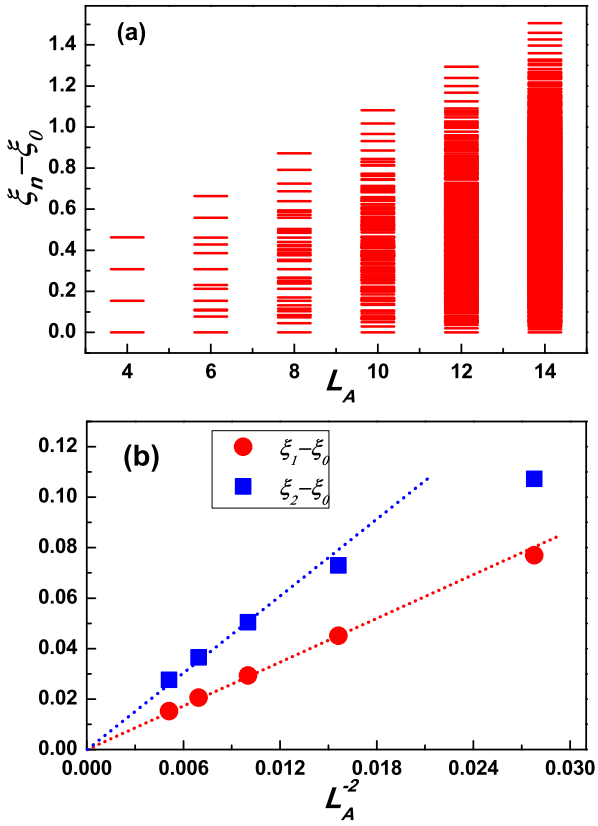

FIG. 4: (a) The bulk ES with $S = 1$ and the block length $l = 3$, the lowest level is $(L_A + 1)$-fold degenerate. (b) The entanglement spectral gap is linear with square of the inverse subsystem size, indicating a spin-wave excitation for the ferromagnetic Heisenberg spin chain. The second excited level is also plotted, but the data from small sizes slightly deviate from the line.

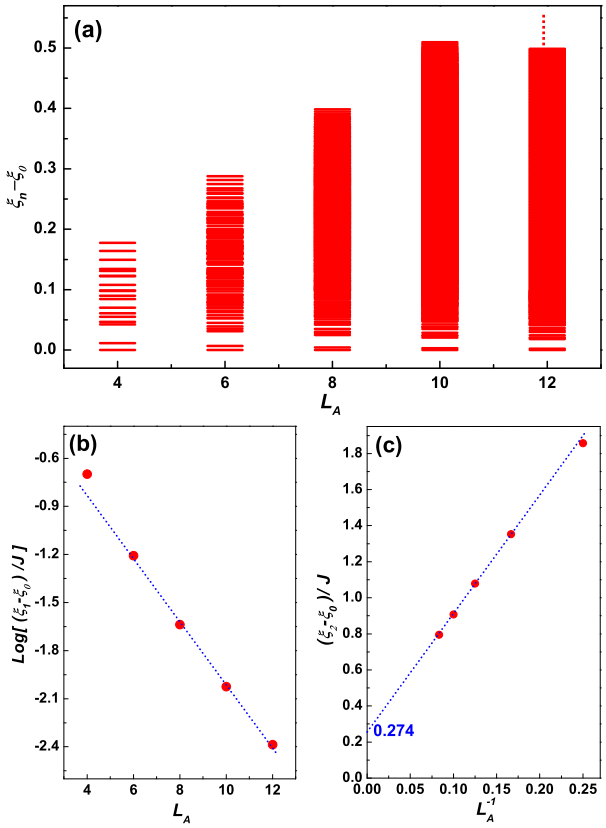

FIG. 5: (a) The bulk ES with $S = 2$ and the block length $l = 6$ for an open chain. The lowest level is singlet, and the first excited level is triplet. (b) The first excited level decays exponentially with the subsystem size. (c) The bulk excitation energy $(\xi_2 - \xi_0)/J\,(l)$ saturates to a finite value in thermodynamic limit.

the density matrix renormalization group calculation[26]. The difference can be improved when the longer length of the effective spin chain is calculated.

V. DISCUSSION AND CONCLUSION

The symmetric bulk bipartition allows us to establish a general description of QCP separating the SPT phase from its trivial gapped phase *directly* from the fixed point wave function of the topological phase. Any asymmetric bulk partition for the AKLT wave function always leads to a bulk ES with multiple gaps (see Appendix C). For the one-dimensional SPT phase with the protecting symmetry of $G = SO(3)$ Lie group, its fundamental group is $\Pi_1(G) = Z_2$. So there are only two different phases: the odd integer spin Haldane gapped phase and its trivial gapped phase adiabatically connected to the even integer spin Haldane gapped phase. A QCP exists to separate these two phases, and the effective model Hamiltonian for this QCP is just given by the quantum antiferromagnetic Heisenberg half-odd integer spin chain. The corresponding critical theory is characterized by the 1+1 (space-time) dimensional $SU(2)_1$ WZW conformal field theory with the Lie group $\tilde{G} = SU(2)$, where $\tilde{G}$ is just the universal covering group of G and has a trivial fundamental group, $\Pi_1(\tilde{G}) = 1$. Our results may thus generalize the widely discussed bulk-edge correspondence: the bulk topological property of the topological phase not only determines its symmetry-protected edge degrees of freedom, but also the critical properties of the second order phase transition to the trivial phase. Furthermore, the fundamental degrees of freedom of the critical theory are precisely these edge degrees of freedom *confined* in the bulk of the topological phase. As a result this QCP is a typical deconfined critical point. These results can be generalized for other SPT phases with the protecting symmetry of continuous Lie group.

To summarize, we have applied a symmetric bulk bipartition to the one-dimensional AKLT VBS states for the integer spin-S Haldane gapped phase, and an array of fractionalized spin-S/2 edge spins can be created in the reduced bulk system. Via the calculations of the

bulk entanglement spectra for the reduced system, the topological properties encoded in the original VBS wave functions are revealed.

Acknowledgements.- G. M. Zhang would like to thank D. H. Lee and X. Wan for the helpful discussions and acknowledge the support of NSF-China through Grant No.20121302227. K. Yang is supported by NSF grants DMP-1442366 and DMP-1157490.

APPENDIX A: ENTANGLEMENT HAMILTONIAN OF THE SPIN-1 AKLT STATE

The simplest example of the SPT phase is the Haldane gapped phase of the SO(3) symmetric antiferromagnetic spin-1 chain, whose fixed point ground state wave function is given by the AKLT matrix product state

$$|\psi\rangle = \sum_{\{s_i\}} \mathrm{Tr}\left(\mathbf{A}^{[s_1]}\mathbf{A}^{[s_2]}...\mathbf{A}^{[s_N]}\right)|s_1,s_2,...s_N\rangle\,, \quad (14)$$

$$A^{[1]} = \sqrt{\frac{1}{3}}\tau^+, A^{[0]} = -\sqrt{\frac{1}{3}}\tau^z, A^{[-1]} = -\sqrt{\frac{1}{3}}\tau^-,$$

where the local spin $s_i = -1, 0, 1$ and $\tau^\pm = (\tau^x \pm i\tau^y)/\sqrt{2}$ as the Pauli matrices. In the thermodynamic limit, the spin-spin correlation function decays exponentially with a correlation length $\xi = 1/\ln 3$. When we make a cut in real space, the periodic spin chain transforms into an open chain with fractionalized spin-1/2 edge spins. For a sufficiently long length, these two edge spins are almost free, leading to four degenerate ground states. The degenerate ground state has a residual entropy per edge given by $s_r = \ln 2$.

If a block of l spins ($l \geq 2$) is chosen as a subsystem A in the state, its reduced density matrix and eigenvalues can be calculated easily, and the levels in the entanglement spectrum (ES) are given by

$$\xi_0 = \ln 4 - \ln\left[1 + 3\left(-\frac{1}{3}\right)^l\right],$$
$$\xi_1 = \ln 4 - \ln\left[1 - \left(-\frac{1}{3}\right)^l\right]. \quad (15)$$

So when the block contains even number of lattice sites, the lowest level is singlet and the excited one is triplet, while the entanglement levels switch each other for the odd number of lattice sites included in the block. For a sufficient long block, these four entanglement levels become nearly degenerate, and the entanglement spectrum can be captured by the following entanglement Hamiltonian (EH),

$$H_b = 4\left(-\frac{1}{3}\right)^l \mathbf{s}_R \cdot \mathbf{s}_L, \quad (16)$$

where $\mathbf{s}_R$ and $\mathbf{s}_L$ denote the edge spin-1/2's of the block and the coupling strength exponentially depends on the length of the block.

Actually, such a bipartition scheme can be generalized to the bulk partition with a large number of disjoint blocks with alternating lengths l_A and l_B, yielding an extensive number of fractionalized edge spins in the reduced bulk subsystem. However, the symmetric bulk bipartition ($l_A = l_B = l$) is only the most important because any asymmetric bipartition leads to a gapped ES. To rewrite the wave function into block form, we introduce an auxiliary tensor and perform singular value decomposition

$$\left(A^{[s_1]}A^{[s_2]}..A^{[s_l]}\right)_{\alpha,\beta} = \sum_{p=0}^{\kappa-1} X_{(\{s_i\}),p}\Lambda_p Y_{p,(\alpha,\beta)}, \quad (17)$$

where the number of non-zero values $\kappa = 4$ records the number of singular states in each block, formed by two edge spin-1/2's. When we express the block basis as

$$|p\rangle = \sum_{\{m_1,m_2\}=0}^{1} \chi^p_{m_1,m_2}|m_1,m_2\rangle, \quad (18)$$

with $\chi^0 = i\tau^y/\sqrt{2}$,$\chi^1 = \left(\tau^0 + \tau^z\right)/2$, $\chi^2 = \tau^x/\sqrt{2}$, and $\chi^3 = \left(\tau^0 - \tau^z\right)/2$, the wave function is able to be expressed in terms of block matrices

$$|\psi\rangle = \sum_{\{p_i\}} \mathrm{Tr}\left(B^{[p_1]}B^{[p_2]}..B^{[p_{N/l}]}\right)|p_1,p_2,..p_{N/l}\rangle,$$

with

$$B^{[0]} = -\frac{\sqrt{1+3\delta}}{2}\tau^0, B^{[1]} = \frac{\sqrt{1-\delta}}{2}\tau^+$$
$$B^{[2]} = -\frac{\sqrt{1-\delta}}{2}\tau^z, B^{[3]} = -\frac{\sqrt{1-\delta}}{2}\tau^- \quad (19)$$

and $\delta = \left(-\frac{1}{3}\right)^l$.

To generate a bulk ES, we have to make extensive bipartition by denoting all the even blocks as the subsystem A and the odd blocks as subsystem B. Clearly A and B is symmetric with each other under inversion operation. When we trace out the subsystem B, the reduced density matrix can be written into the matrix product form shown in Fig.2c,

$$\rho_A = \sum_{\{p_i,q_i\}} \mathrm{Tr}\left(\prod_i \rho^{[p_i,q_i]}\right)|p_1\rangle\langle q_1| \otimes |p_2\rangle\langle q_2|..|p_{N/l}\rangle\langle q_{N/l}| \quad (20)$$

where the repeating tensor is

$$R_j = \sum_{\{p_j,q_j\}} \left[\left(B^{[p_j]} \otimes \overline{B}^{[q_j]}\right)T\right]|p_j\rangle\langle q_j|, \quad (21)$$

where T is the blocked transfer matrix.

To extract the entanglement Hamiltonian H_E, we have to rewrite the projection operator $|p\rangle\langle q|$ in the basis of

$\sigma^{\alpha_L}\otimes\sigma^{\alpha_R}$, where $\sigma^0=1$ and $\sigma^\alpha\,(\alpha=1,2,3)$ as Pauli matrices. Then the repeating structure of ρ_A changes into

$$R_j = \sum_{\{p,q\}}\sum_{\{m,n,\alpha\}=0}^{1}\left[\left(B^{[p_j]}\otimes\overline{B}^{[q_j]}\right)T\right]\chi^{p_j}_{m_1,m_2}\overline{\chi}^{q_j}_{n_1,n_2} \times\Gamma_{(m_1,n_1),\alpha_{2j-1}}\Gamma_{(m_2,n_2),\alpha_{2j}}\sigma^{\alpha_{2j-1}}\otimes\sigma^{\alpha_{2j}} \quad (22)$$

where the matrix Γ has been used

$$\Gamma=\frac{1}{4}\begin{bmatrix}2\tau^0 & \sqrt{2}\left(\tau^+ + i\tau^-\right)\\ 2\tau^x & (1-i)\,\tau^z-(1+i)\,\tau^0\end{bmatrix}.$$

Although R_j tensor is quite complicated, a unitary transformation

$$U=\frac{1}{\sqrt{2}}\begin{bmatrix}\tau^0 & \tau^x\\ -\tau^x & \tau^0\end{bmatrix} \quad (23)$$

can be used to simplify it. Furthermore, for $l\gg 2$, the parameter δ is very small and R_j can be expressed in power series of δ. To the first order of δ, two edge spins of each block decouple, leading to $R_j=\widetilde{R}_{2j-1}\widetilde{R}_{2j}$ with the simplest form

$$\widetilde{R}_j=\frac{1}{2}\begin{bmatrix}1 & -\delta\sigma^x_j & -i\delta\sigma^y_j & \delta\sigma^z_j\\ \sigma^x_j & 0 & 0 & 0\\ -i\sigma^y_j & 0 & 0 & 0\\ -\sigma^z_j & 0 & 0 & 0\end{bmatrix}. \quad (24)$$

In the end, H_E can be derived as

$$H_E=-\log\mathrm{Tr}\left(\prod_j\widetilde{R}_j\right)\approx\left(-\frac{1}{3}\right)^l\sum_j\sigma_j\cdot\sigma_{j+1}, \quad (25)$$

corresponding to the quantum spin-1/2 Heisenberg chain. Depending on the parity of the block length l, the nearest neighbor spin exchange is either antiferromagnetic or ferromagnetic coupling. If the blocks include even number of lattice sites, the corresponding ES reveals an emergent quantum critical state with fractionalized spinons as the low-energy excitations. When the blocks include odd number of lattice sites, however, the resulting bulk ES features ferromagnetic long-range order and spin wave excitations. To the higher order of δ, the edge spin decoupling in R_j does not hold and the EH includes longer range spin exchange couplings. However, the coupling strengths of these terms are exponentially small, irrelevant to the low-energy excitations.

APPENDIX B: ENTANGLEMENT HAMILTONIAN OF THE SPIN-2 AKLT STATE

Our extensive bipartition scheme can be applied to any MPS state, the resulting entanglement Hamiltonian describes the percolation between edge spins. Let us consider the spin-2 AKLT state and its MPS wave function is defined by

$$|\psi\rangle=\sum_{\{s_i\}=-2}^{2}\mathrm{Tr}\left[A^{[s_1]}A^{[s_2]}..A^{[s_N]}\right]|s_1,s_2,..s_N\rangle, \quad (26)$$

where the local matrices are given by

$$\begin{aligned}A^{[-2]} &= \sqrt{\frac{3}{5}}\begin{bmatrix}0&0&0\\0&0&0\\1&0&0\end{bmatrix}, A^{[-1]}=\sqrt{\frac{3}{10}}\begin{bmatrix}0&0&0\\-1&0&0\\0&1&0\end{bmatrix},\\ A^{[1]} &= \sqrt{\frac{3}{10}}\begin{bmatrix}0&1&0\\-1&0&0\\0&0&0\end{bmatrix}, A^{[2]}=\sqrt{\frac{3}{5}}\begin{bmatrix}0&0&1\\0&0&0\\0&0&0\end{bmatrix},\\ A^{[0]} &= \frac{1}{\sqrt{10}}\begin{bmatrix}1&0&0\\0&-2&0\\0&0&1\end{bmatrix}.\end{aligned} \quad (27)$$

In this state, each physical site localizes two spin-1's, they tensor together into the spin-2 subspace, and each pair of neighboring sites is linked with spin-1 singlet. In the thermodynamic limit, the spin-spin correlation function decays exponentially with a correlation length $\xi=1/\ln 2$. When a cut is made in real space, the periodic spin chain transforms into an open chain with two spin-1 edge spins. For a sufficiently long length, these two edge spins are almost free, leading to nine degenerate ground states. The degenerate ground state has a residual entropy per edge given by $s_r=\ln 3$. This wave function describes the fixed point state of the spin-2 Haldane gapped phase. Since the spin-1 edge spins have a faithful representation of SO(3) group, this gapped phase is believed to be adiabatically connected to the trivial state.

To gain some insight about the bulk entanglement Hamiltonian, we first consider a single block case. Analytical result of block ES can be obtained by means of spin coherent state path integral, the eigenvalues of single length-l block reduced density matrix are

$$\begin{aligned}\lambda_0 &= \frac{1}{9}\left[1+3\left(-\frac{1}{2}\right)^l+5\left(\frac{1}{10}\right)^l\right],\\ \lambda_1 &= \frac{1}{9}\left[1+\frac{3}{2}\left(-\frac{1}{2}\right)^l-\frac{5}{2}\left(\frac{1}{10}\right)^l\right],\\ \lambda_2 &= \frac{1}{9}\left[1-\frac{3}{2}\left(-\frac{1}{2}\right)^l+\frac{1}{2}\left(\frac{1}{10}\right)^l\right],\end{aligned} \quad (28)$$

corresponding to singlet, triplet and quintet, respectively. The entanglement Hamiltonian can be readily obtained as

$$\begin{aligned}H_b &= \frac{3}{2}\left[\left(-\frac{1}{2}\right)^l-\frac{3}{8}\left(-\frac{1}{2}\right)^{2l}\right](\mathbf{s}_1\cdot\mathbf{s}_2)\\ &\quad-\frac{3}{2}\left[\left(\frac{1}{10}\right)^l-\frac{3}{8}\left(-\frac{1}{2}\right)^{2l}\right](\mathbf{Q}_1\cdot\mathbf{Q}_2),\end{aligned} \quad (29)$$

where $\mathbf{s}_i$ are spin-1 dipole and $\mathbf{Q}_i$ are quadruple of the edge spins with the definitions

$$\begin{aligned} Q^1 &= (s^x)^2-(s^y)^2, Q^2=\frac{1}{\sqrt{3}}\left[3(s^z)^2-2\right], \\ Q^3 &= \{s^y,s^z\}, Q^4=\{s^z,s^x\}, Q^5=\{s^x,s^y\}. \end{aligned}$$

For $l \gg 1$, we have

$$H_b \approx \frac{3}{2}\left(-\frac{1}{2}\right)^l (\mathbf{s}_L \cdot \mathbf{s}_R). \quad (30)$$

We now derive the entanglement Hamiltonian under symmetric bulk bipartition. When conducting the same coarse graining to this state, for a general l-site ($l \geq 2$) block, we will end with 9 relevant states

$$|p\rangle = \sum_{\{m_1,m_2\}=-1}^{1} \chi^p_{m_1,m_2}|m_1,m_2\rangle. \quad (31)$$

Introduce

$$K = \frac{1}{\sqrt{2}}\begin{bmatrix} 0 & 0 & 1 \\ 0 & -1 & 0 \\ 1 & 0 & 0 \end{bmatrix}, \quad (32)$$

the exact form of χ^p can be brought into the compact form

$$\begin{aligned} \chi^0 &= \sqrt{2}K/\sqrt{3}, \chi^1 = s^- K, \chi^2 = s^z K, \chi^3 = s^+ K \\ \chi^4 &= \left(Q^1 - iQ^5\right)K/\sqrt{2}, \chi^5 = \left(Q^4 - iQ^3\right)K, \chi^6 = Q^3 K \\ \chi^7 &= \left(-Q^4 - iQ^3\right)K, \chi^8 = \left(Q^1 + iQ^5\right)K/\sqrt{2}, \end{aligned} \quad (33)$$

with $s^{\pm} = \left(s^x \pm is^y\right)/\sqrt{2}$. Then the VBS wave function is able to be expressed in terms of block matrices as

$$|\psi\rangle = \sum_{\{p_i\}} \mathrm{Tr}\left(B^{[p_1]}B^{[p_2]}..B^{\left[p_{N/l}\right]}\right)|p_1,p_2,..p_{N/l}\rangle, \quad (34)$$

with the block matrices

$$\begin{aligned} B^{[0]} &= \sqrt{\lambda_0}, B^{[1]} = \sqrt{3\lambda_1/2}s^-, B^{[2]} = \sqrt{3\lambda_1/2}s^z, \\ B^{[3]} &= -\sqrt{3\lambda_1/2}s^+, B^{[4]} = \sqrt{3\lambda_2/4}\left(Q^1 - iQ^5\right), \\ B^{[5]} &= -i\sqrt{3\lambda_2/4}\left(Q^3 + iQ^4\right), B^{[6]} = \sqrt{3\lambda_2/2}Q^2, \\ B^{[7]} &= -i\sqrt{3\lambda_2/4}\left(Q^3 - iQ^4\right), B^{[8]} = \sqrt{3\lambda_2/4}\left(Q^1 + iQ^5\right). \end{aligned}$$

The reduced density matrix is also in the MPO form, that is

$$\begin{aligned} \rho_A &= \mathrm{Tr}\left(\prod_j R_j\right), \\ R_j &= \sum_{\{p_j,q_j\}}\left[\left(B^{[p_j]}\otimes\overline{B}^{[q_j]}\right)T\right]|p_j\rangle\langle q_j|, \end{aligned} \quad (35)$$

Here we also have to expand the projection operator in terms of spin operators,

$$|m\rangle\langle n| = \sum_{\alpha=0}^{8}\Gamma_{(m,n),\alpha}O^\alpha, \quad (36)$$

where $\overrightarrow{O} = \left\{\mathbf{1}, \overrightarrow{s}, \overrightarrow{Q}\right\}$ are the nine operators. The exact form of Γ is found to be

$$\Gamma = \begin{bmatrix} \frac{1}{3} & 0 & 0 & -\frac{1}{2} & 0 & \frac{1}{2\sqrt{3}} & 0 & 0 & 0 \\ 0 & \frac{1}{2\sqrt{2}} & -\frac{i}{2\sqrt{2}} & 0 & 0 & 0 & \frac{i}{2\sqrt{2}} & -\frac{1}{2\sqrt{2}} & 0 \\ 0 & 0 & 0 & 0 & \frac{1}{2} & 0 & 0 & 0 & -\frac{i}{2} \\ 0 & \frac{1}{2\sqrt{2}} & \frac{i}{2\sqrt{2}} & 0 & 0 & 0 & -\frac{i}{2\sqrt{2}} & -\frac{1}{2\sqrt{2}} & 0 \\ \frac{1}{3} & 0 & 0 & 0 & 0 & -\frac{1}{\sqrt{3}} & 0 & 0 & 0 \\ 0 & \frac{1}{2\sqrt{2}} & -\frac{i}{2\sqrt{2}} & 0 & 0 & 0 & -\frac{i}{2\sqrt{2}} & \frac{1}{2\sqrt{2}} & 0 \\ 0 & 0 & 0 & 0 & \frac{1}{2} & 0 & 0 & 0 & \frac{i}{2} \\ 0 & \frac{1}{2\sqrt{2}} & \frac{i}{2\sqrt{2}} & 0 & 0 & 0 & \frac{i}{2\sqrt{2}} & \frac{1}{2\sqrt{2}} & 0 \\ \frac{1}{3} & 0 & 0 & \frac{1}{2} & 0 & \frac{1}{2\sqrt{3}} & 0 & 0 & 0 \end{bmatrix}$$

Also in this case we have to make use the gauge freedom, we find it's convenient to introduce the following transformation matrix

$$U = \begin{bmatrix} \frac{1}{\sqrt{3}} & 0 & 0 & 0 & \frac{1}{\sqrt{3}} & 0 & 0 & 0 & \frac{1}{\sqrt{3}} \\ -\sqrt{\frac{5}{8}} & 0 & 0 & 0 & 0 & 0 & 0 & 0 & \sqrt{\frac{5}{8}} \\ 0 & \frac{1}{2} & 0 & \frac{1}{2} & 0 & \frac{1}{2} & 0 & \frac{1}{2} & 0 \\ 0 & -\frac{1}{2} & 0 & \frac{1}{2} & 0 & -\frac{1}{2} & 0 & \frac{1}{2} & 0 \\ \frac{\sqrt{5}}{6} & 0 & 0 & 0 & -\frac{\sqrt{5}}{3} & 0 & 0 & 0 & \frac{\sqrt{5}}{6} \\ 0 & -\frac{1}{2} & 0 & -\frac{1}{2} & 0 & \frac{1}{2} & 0 & \frac{1}{2} & 0 \\ 0 & 0 & \frac{1}{\sqrt{2}} & 0 & 0 & 0 & \frac{1}{\sqrt{2}} & 0 & 0 \\ 0 & \frac{1}{2} & 0 & -\frac{1}{2} & 0 & -\frac{1}{2} & 0 & \frac{1}{2} & 0 \\ 0 & 0 & -\frac{1}{\sqrt{2}} & 0 & 0 & 0 & \frac{1}{\sqrt{2}} & 0 & 0 \end{bmatrix}$$

Then after the same procedure the repeating structure R_j is got. Like in the spin-1 AKLT case, first we only keep the $\delta = \left(-\frac{1}{2}\right)^l$ order term, the two sites in one block decouple into $\widetilde{R}_{2j-1}\widetilde{R}_{2j}$ in this order, thus the translational invariance is restored. The form of $\widetilde{R}_j$ is

$$\widetilde{R}_j \approx \frac{1}{\sqrt{6}}\begin{bmatrix} \sqrt{2/3} & -2\delta O^3_j/\sqrt{5} & -\delta O^1_j & i\delta O^2_j & 0 & 0 & 0 & 0 & 0 \\ \sqrt{5}O^3_j/2 & 0 & 0 & 0 & 0 & 0 & 0 & 0 & 0 \\ O^1_j & 0 & 0 & 0 & 0 & 0 & 0 & 0 & 0 \\ iO^2_j & 0 & 0 & 0 & 0 & 0 & 0 & 0 & 0 \\ \sqrt{5/6}O^5_j & 0 & 0 & 0 & 0 & 0 & 0 & 0 & 0 \\ O^7_j & 0 & 0 & 0 & 0 & 0 & 0 & 0 & 0 \\ O^4_j & 0 & 0 & 0 & 0 & 0 & 0 & 0 & 0 \\ iO^6_j & 0 & 0 & 0 & 0 & 0 & 0 & 0 & 0 \\ iO^8_j & 0 & 0 & 0 & 0 & 0 & 0 & 0 & 0 \end{bmatrix}. \quad (37)$$

It can then be concluded, to the first order of δ

$$\begin{aligned} \rho_A &= \mathrm{Tr}\left(\prod_j \widetilde{R}_j\right) = \frac{1}{3^N}\left(1 - \frac{3}{2}\delta\sum_j \mathbf{s}_j \cdot \mathbf{s}_{j+1}\right) \\ H_E &\approx \frac{3}{2}\left(-\frac{1}{2}\right)^l \sum_j \mathbf{s}_j \cdot \mathbf{s}_{j+1}. \end{aligned} \quad (38)$$

When l is taken to be even, the Heisenberg interaction is generated, thus an Haldane phase spectrum appears. When higher order terms gets involved, the decoupling of R_j does not hold, and there will be both long range interaction terms and quadruple interaction terms appear in H_E, they both become irrelevant, thus the universality class of H_E is determined by the Heisenberg interaction.

APPENDIX C: ASYMMETRIC BULK BIPARTITION

Under asymmetric bulk bipartition, the interaction strengths between spin-$S/2$ within one block and adjacent blocks can differ dramatically. As a result, the translational invariance is broken, and the EH reduces to the $J_1 - J_2$ quantum Heisenberg model of spin-$S/2$ chain

$$H_E = \sum_i \left[J_1 \left(l_A \right) \mathbf{s}_{2j-1} \cdot \mathbf{s}_{2j} + J_2 \left(l_B \right) \mathbf{s}_{2j} \cdot \mathbf{s}_{2j+1} \right]. \quad (39)$$

where $J_1 \left(l_A \right) = \frac{12}{S(S+2)} \left(\frac{-S}{S+2} \right)^{l_A}$ and $J_2 \left(l_B \right) = \frac{12}{S(S+2)} \left(\frac{-S}{S+2} \right)^{l_B}$. When both l_A and l_B are even, the H_E can be brought into the standard spin dimerized model

$$H_E = J \sum_i \left[1 + \delta \left(-1 \right)^i \right] \mathbf{s}_i \cdot \mathbf{s}_{i+1}, \quad (40)$$

with the dimerization parameter

$$\delta = \frac{1 - \left(-\frac{S}{S+2} \right)^{|l_A - l_B|}}{1 + \left(-\frac{S}{S+2} \right)^{|l_A - l_B|}}. \quad (41)$$

In $S = 1$ case, the Lieb-Schulz-Mattice theorem governs that a dimerized phase spectrum will always emerge. Thus, when the bipartition is switched from symmetric to asymmetric, a phase transition in the resulting bulk ES will occur. However, we can not tune the asymmetric parameter $|l_A - l_B|$ continuously, because the smallest value is 2. Hence we can not approach the critical point, which enforces that the critical point is a deconfined one. To get an intuitive picture of the dimerized bulk ES, we choose the special cases with $(l_A, l_B) = (2,2), (4,2), (6,2), (8,2)$, and pick out the resulting bulk ES for $L_A = 12$ displayed in Fig. 6. We can see that as the asymmetry becomes large, the bulk ES becomes a multilevel structure with equal spacing, where the coupling constant J_1 is negligible compared to J_2. Then the reduced subsystem A consists of total isolated $L_A/2$ unit cells. Therefore, the degeneracy of the n-th level is expected to be $3C^n_{L_A/2}$ and $n = \{1, 2, ..L_A/2 + 1\}$, which has been confirmed by the numerical result. Even in the $S = 2$ AKLT case, the minimal dimerization parameter is $\delta = 3/5$ for $|l_A - l_B| = 2$. This also exceeds the critical value for the Haldane-dimerized transition point $\delta_c \simeq 0.255$.

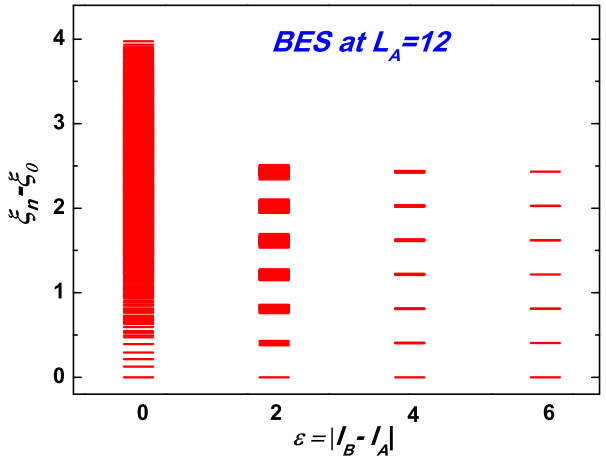

FIG. 6: The bulk ES with $L_A = 12$ for different asymmetric bipartition $\varepsilon = |l_A - l_B|$. There is a transition from critical spectrum to the dimerized phase. Since the smallest value of $|l_A - l_B|$ is 2, our bulk bipartition method can not approach continuously to the critical value.

* Electronic address: gmzhang@tsinghua.edu.cn

[1] D. J. Thouless, M. Kohmoto, M. P. Nightingale, and M. den Nijs, Phys. Rev. Lett. 49, 405 (1982).

[2] M. Z. Hasan and C. L. Kane, Rev. Mod. Phys. **82**, 3045 (2010).

[3] X. L. Qi and S. C. Zhang, Rev. Mod. Phys. **83**, 1057 (2011).

[4] J. E. Moore, Nature (London) **464**, 194 (2010).

[5] X. Chen, Z. C. Gu, and X. G. Wen, Phys. Rev. B **83**, 035107 (2011).

[6] N. Schuch, D. Perez-Garcia, and I. Cirac, Phys. Rev. B **84**, 165139 (2011).

[7] X. Chen, Z. C. Gu, Z. X. Liu, and X. G. Wen, Phys. Rev. B **87**, 155114 (2013).

[8] X. Chen, F. Wang, Y. M. Lu, and D. H. Lee, Nucl. Phys. B **873** (FS) 248 (2013).

[9] W. J. Rao, X. Wan, and G. M. Zhang,Phys. Rev. B **90**, 075151 (2014).

[10] T. H. Hsieh, L. Fu, X. L. Qi, Phys. Rev. B **90** , 085137 (2014); T. H. Hsieh and L. Fu, Phys. Rev. Lett. **113**, 106801 (2014).

[11] L. Tsui, Y. M. Lu, H. C. Jiang, and D. H. Lee, Nucl. Phys. B **896** (FS) 330 (2015); L. Tsui, F. Wang and D. H. Lee, arXiv:1511.07460.

[12] T. Senthil, A. Vishwanath, L. Balents, S. Sachdev, and M. P. A. Fisher, Science **303**, 1490 (2004).

[13] F. D. M. Haldane, Phys. Lett. **93A**, 464 (1983); Phys. Rev. Lett. **50**, 1153 (1983).

[14] Z. C. Gu and X. G. Wen, Phys. Rev. B **80**, 155131 (2009).

[15] F. Pollmann, E. Berg, A. M. Turner, and M. Oshikawa, Phys. Rev. B **85**, 075125 (2012).

[16] I. Affleck, T. Kennedy, E. H. Lieb, and H. Tasaki, Phys. Rev. Lett. **59**, 799 (1987); Commun. Math. Phys. **115**, 477 (1988).

[17] W. J. Rao, K. Cai, X. Wan, and G. M. Zhang, Phys. Rev. B **92**, 214430 (2015).

[18] R. A. Santos, C. M. Jian, and R. Lundgren, arXiv:1511.01489.

[19] H. Katsura, T. Hirano, and Y. Hatsugai, Phys. Rev. B **76**, 012401 (2007).

[20] V. E. Korepin and Y. Xu, Int. J. Modern Phys. B **24**, 1361 (2010).

[21] F. Verstraete, J. I. Cirac, J. I. Latorre, E. Rico, and M. M. Wolf,Phys. Rev. Lett. **94**, 140601(2005).

[22] I. Affleck and F. D. M. Haldane, Phys. Rev. B **36**, 5291 (1987).
[23] S. C. Furuya and M. Oshikawa, arXiv:1503.07292.
[24] P. Calabrese and J. Cardy, J. Phys. A **42**, 504005 (2009).
[25] A. Kitazawa and K. Nomura, Phys. Rev. B **59**, 11358 (1999).
[26] S. R. White, Phys. Rev. Lett. **69**, 2863 (1992).